Chapter 4

Numerical Analysis

In this chapter the numerical techniques as described in the previous chapter are compared and analysed in detail. Initially, the CV-UM vertex based FVM and the Bubnov-Galerkin FEM are shown to be equivalent for an academic one dimensional comparison. Next, the two techniques are compared and analysed for the two dimensional case with a full description of the computational elements in both cases. Finally, the three dimensional implementations are also compared and analysed again in both cases. In the remaining chapter, the Bubnov-Galerkin FEM will be simply referred to as the FEM and the CV-UM vertex based FVM will be simply referred to as the FVM.

4.1 Theoretical analysis of discretisation

In this section, the FVM and the FEM will be analysed and compared in detail. The analysis and comparison is performed in a one, two and three dimensional context. In each case, the similarities and differences of the two methods are described.

As visco-plasticity is time dependent, a time stepping scheme must be introduced in order to describe the situation numerically. A time stepping scheme allows the solution to march

through the instances in time t_n and t_{n+1} using the time step Δt_n as follows:

$$t_{n+1} = t_n + \Delta t_n,$$

where the subscripts denote successive time steps. A number of time stepping schemes are available as described in the previous chapter, the simple Euler method is adopted for this analysis. Using the Euler method it is possible to integrate the visco-plastic strain rate vector over a time step and obtain the following visco-plastic strain increment vector;

$$\Delta \boldsymbol{\epsilon}_n^{vp} = \dot{\boldsymbol{\epsilon}}_n^{vp} \Delta t_n.$$

From this integration the total visco-plastic strain vector

$$\boldsymbol{\epsilon}_{n+1}^{vp} = \boldsymbol{\epsilon}_n^{vp} + \Delta \boldsymbol{\epsilon}_n^{vp},$$

occurring at the time instant t_{n+1}, is obtained. Having obtained the total visco-plastic strain vector, it is now possible to perform a numerical analysis of a visco-plastic problem.

4.1.1 One Dimensional Analysis

The one dimensional analysis is presented in order to compare the two approaches in their simplest forms. A one dimensional approach is not practical for the numerical applications in this research, but it is useful from a theoretical viewpoint.

The problem illustrated in Figure 4.1 consists of a one dimensional, two noded element with linear displacement variation. The problem was analyzed for the FEM by Owen and Hinton [72]. Assuming that the total visco-plastic strain is constant over the element, the change of length of this element due to the total visco-plastic strain at time t_{n+1} is

$$u_{n+1} = \epsilon_{n+1}^{vp} L,$$

where ϵ_{n+1}^{vp} is the one dimensional total visco-plastic strain. Including the additional change in length due to the applied load at a node p_{n+1}, occurring at the time instant t_{n+1}, gives

$$u_{n+1} = \epsilon_{n+1}^{vp} L + \frac{L}{AE} p_{n+1}, \tag{4.1}$$

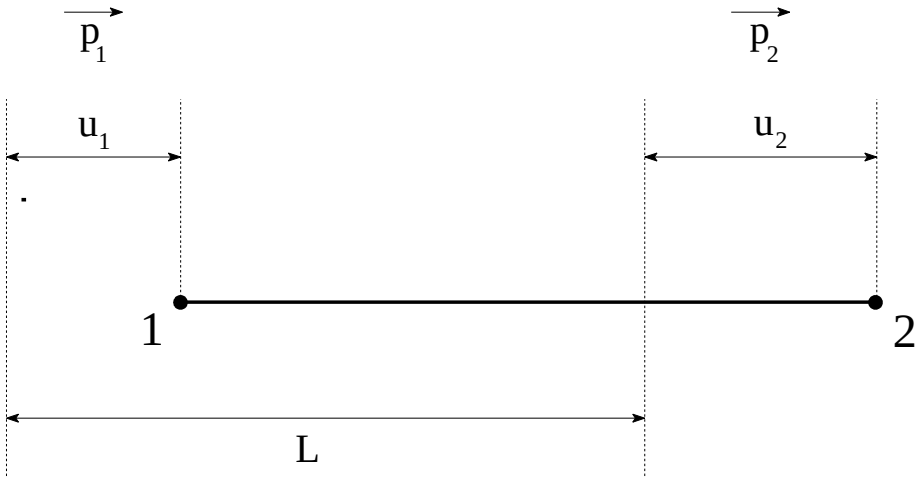

Figure 4.1: One dimensional, two noded element.

where E is Young's modulus, A is the cross-sectional area and L is the element length. Equation (4.1) can be expressed in matrix form,

$$\mathbf{u}_{n+1} = \mathbf{K}^{-1}\mathbf{f}_{n+1},$$

where the displacements and nodal forces are

$$\begin{aligned} \mathbf{u}_{n+1} &= \begin{bmatrix} u_1 \\ u_2 \end{bmatrix}_{n+1}, \\ \mathbf{f}_{n+1} &= AE\epsilon^{vp}_{n+1}\begin{bmatrix} 1 \\ -1 \end{bmatrix} + \begin{bmatrix} p_1 \\ p_2 \end{bmatrix}_{n+1} \end{aligned} \tag{4.2}$$

and the elemental stiffness matrix is

$$\mathbf{K}^e = \frac{EA}{L}\begin{bmatrix} 1 & -1 \\ -1 & 1 \end{bmatrix}. \tag{4.3}$$

It should be noted that $\mathbf{K}^e$ cannot be inverted directly in the present form, but if a fixed displacement is applied to the single element or element assembly form then inversion is possible as the matrix then becomes non-singular.

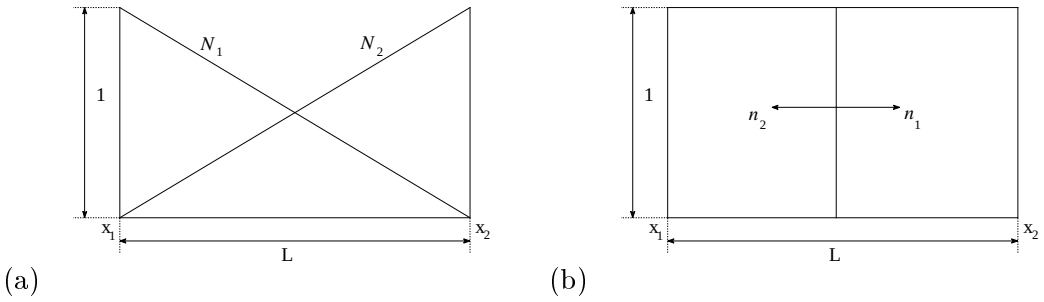

Figure 4.2: 1D (a) shape functions and FEM weighting functions, (b) FVM weighting functions.

The expressions obtained by the previous one dimensional analysis can be obtained directly from the FEM and the FVM. This can be achieved using the simplified elemental versions of the general FEM equations (3.19) and (3.20),

$$\begin{aligned} \mathbf{K}_e^{\text{fe}} &= \int_v \mathbf{B}^{\mathbf{T}}\mathbf{D}\mathbf{B}dv, \\ \mathbf{f}_{n+1}^{\text{fe}} &= -\int_v \mathbf{B}^{\mathbf{T}}\mathbf{D}\epsilon_{n+1}^{vp}dv + \mathbf{p}_{n+1} \end{aligned} \tag{4.4}$$

and the simplified elemental versions of the general FVM equations (3.22) and (3.23)

$$\begin{aligned} \mathbf{K}_e^{\text{fv}} &= -\int_s \mathbf{R}^{\mathbf{T}}\mathbf{D}\mathbf{B}ds, \\ \mathbf{f}_{n+1}^{\text{fv}} &= \int_s \mathbf{R}^{\mathbf{T}}\mathbf{D}\epsilon_{n+1}^{vp}ds + \mathbf{p}_{n+1}. \end{aligned} \tag{4.5}$$

Surface tractions, thermal strains and body forces are neglected in equations (4.4) and (4.5) for simplicity.

For the one dimensional case described in Figure 4.1

$$\begin{aligned} \int_v dv &= AL, \\ \int_s ds &= A, \\ \mathbf{D} &= E. \end{aligned}$$

The displacement variation is assumed linear and can be described by shape functions of the following form:

$$\mathbf{N} = \begin{bmatrix} N_1 \\ N_2 \end{bmatrix} = \begin{bmatrix} \dfrac{x_2 - x}{L} \\ \dfrac{x - x_1}{L} \end{bmatrix}.$$

The shape functions are illustrated in Figure 4.2(a) and are used to approximate the displacement derivative in both the FEM and the FVM. They are also equivalent to the weighting functions in the FEM. For the one dimensional case $\mathbf{L} = d/dx$ and using equation (3.21)

$$\mathbf{B} = \mathbf{LN} = \begin{bmatrix} -1/L \\ 1/L \end{bmatrix}. \tag{4.6}$$

Also, the normal operator

$$\mathbf{R} = \begin{bmatrix} n_1 \\ n_2 \end{bmatrix} = \begin{bmatrix} \cos\alpha_1 \\ \cos\alpha_2 \end{bmatrix} = \begin{bmatrix} 1 \\ -1 \end{bmatrix}, \tag{4.7}$$

where α is the angle of the outward normal with respect to the one dimensional coordinate, in this case x. The normals and the weighting functions for the FVM are illustrated in Figure 4.2(b).

It is now possible to substitute $\mathbf{B}$ and $\mathbf{R}$ as defined by equations (4.6) and (4.7), respectively, into equations (4.4) and (4.5) relating to the FEM and the FVM, respectively.

Hence,

$$\mathbf{K}_e^{\text{fe}} = \int_v \mathbf{B^T D B} dv = \begin{bmatrix} -1/L & 1/L \end{bmatrix} E \begin{bmatrix} -1/L \\ 1/L \end{bmatrix} AL = \frac{EA}{L} \begin{bmatrix} 1 & -1 \\ -1 & 1 \end{bmatrix}$$

and

$$\mathbf{K}_e^{\text{fv}} = -\int_s \mathbf{R^T D B} ds = -\begin{bmatrix} 1 & -1 \end{bmatrix} E \begin{bmatrix} -1/L \\ 1/L \end{bmatrix} A = \frac{EA}{L} \begin{bmatrix} 1 & -1 \\ -1 & 1 \end{bmatrix}.$$

Similarly, as the total visco-plastic strain is constant over the element

$$\begin{aligned} \mathbf{f}_{n+1}^{\text{fe}} &= -\int_v \mathbf{B^T D} \epsilon_{n+1}^{vp} dv + \mathbf{p}_{n+1} = -\begin{bmatrix} -1/L & 1/L \end{bmatrix} E\epsilon_{n+1}^{vp} AL + \begin{bmatrix} p_1 \\ p_2 \end{bmatrix}_{n+1} \\ &= AE\epsilon_{n+1}^{vp} \begin{bmatrix} 1 \\ -1 \end{bmatrix} + \begin{bmatrix} p_1 \\ p_2 \end{bmatrix}_{n+1} \end{aligned}$$

and

$$\begin{aligned} \mathbf{f}_{n+1}^{\text{fv}} &= \int_s \mathbf{R^T D} \epsilon_{n+1}^{vp} ds + \mathbf{p}_{n+1} = \begin{bmatrix} 1 & -1 \end{bmatrix} E\epsilon_{n+1}^{vp} A + \begin{bmatrix} p_1 \\ p_2 \end{bmatrix}_{n+1} \\ &= AE\epsilon_{n+1}^{vp} \begin{bmatrix} 1 \\ -1 \end{bmatrix} + \begin{bmatrix} p_1 \\ p_2 \end{bmatrix}_{n+1}. \end{aligned}$$

In both cases the resulting equations are directly equivalent to those described by equations (4.2) and (4.3). Hence, the numerical equivalence of the two methods is illustrated with regard to a one dimensional analysis.

4.1.2 Two Dimensional Analysis

Directly equivalent meshes can be handled by the FEM and the FVM, though the stiffness or system matrix contributions are computed differently. The differing elemental contributions per element are illustrated in Figure 4.3 for a general cluster of two dimensional elements surrounding an arbitrary mesh vertex. Figure 4.3(a) illustrates the integration points associated with the elemental contributions for the FVM and Figure 4.3(b) illustrates the Gauss points associated with the elemental contributions for the FEM.

As in the traditional FEM context it is computationally convenient to work in local coordinates so that all elements can be treated identically regardless of how distorted any element may be in terms of global coordinates. The local coordinate systems for triangular and quadrilateral elements are illustrated in Figures 4.4 and Figures 4.7 respectively.

The mapping from local coordinates to global coordinates is performed via shape functions using the standard FEM techniques. The elements described here are isoparametric, thus allowing the shape functions to be utilised for both coordinate transformation and variable approximation. The standard processes of local-global coordinate and derivative transformations as associated with the FEM are described generally in Appendix C, regardless of element type or dimension.

4.1.2.1 Constant strain triangular elements

Directly equivalent shape functions are utilised in the application of both the FEM and the FVM to describe the variation of the displacement (or any other variable) over an element. The shape functions for constant strain triangular (CST) elements are described in Appendix B.

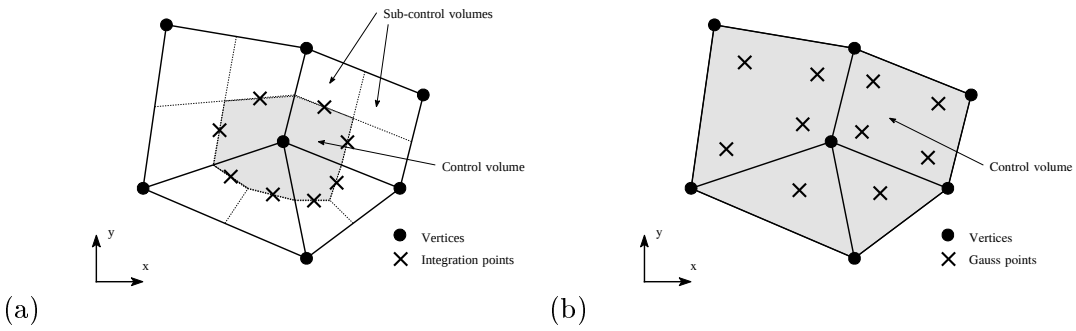

Figure 4.3: Two dimensional integration points (a) FVM and (b) FEM.

The representation of CST elements in local coordinates is illustrated for the FEM and the FVM in Figures 4.4b and 4.4c respectively, both are representations of an arbitrarily deformed CST element in global coordinates as illustrated in Figure 4.4a. In the FEM case the CST element involves one Gauss point, where as in the FVM three integration points are required to construct the associated sub-control volumes.

It is important to note that it is possible to analyse and compare the FVM and the FEM for the CST element due to its simple linear nature. Indeed, it has been shown by Oñate et al [71] that, for elastic problems involving CST elements, the internal force terms contributing to the element stiffness matrix coincide exactly for the FVM and the FEM. Hence, the two methods produce identical stiffness (or coefficient) matrices for two dimensional problems involving CST elements. It should also be noted at this point, that this indicates the general agreement in accuracy between the different integration processes involved in the two methods.

Extending the linear elastic analysis of Oñate et al [71] to problems involving material non-linearity, it can be further shown that the external force terms generated by the visco-plastic strains are also identical for the two methods in the case of two dimensional problem involving CST elements. The visco-plastic terms are described in general for the FEM and FVM in equations 3.20 and 3.23 respectively.

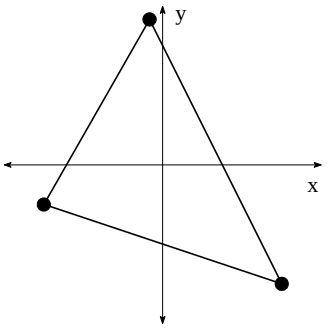

(a)

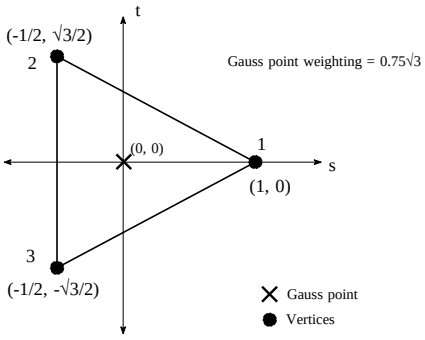

(b)

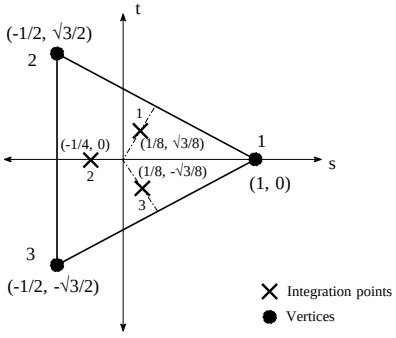

(c)

Figure 4.4: CST element. (a) Global, (b) FEM local and (c) FVM local coordinates.

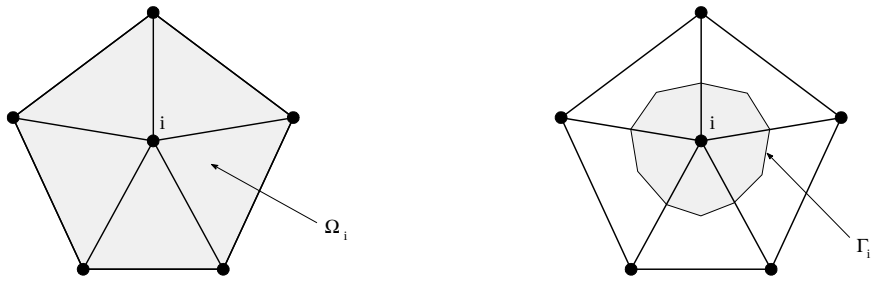

(a) (b)

Figure 4.5: Elemental contributions to the control volume at node i (a) FEM and (b) FVM.

Concentrating on the visco-plastic terms the external force contributions at a node i are

$$\begin{aligned} \mathbf{f}_i^{fe} &= -\int_{\Omega_i} \mathbf{B}_i^{\mathbf{T}} \mathbf{D}\boldsymbol{\epsilon}^{vp}\, d\Omega, \\ \mathbf{f}_i^{fv} &= +\int_{\Gamma_i} \mathbf{R}_i^{\mathbf{T}} \mathbf{D}\boldsymbol{\epsilon}^{vp}\, d\Gamma. \end{aligned} \tag{4.8}$$

for the FEM and the FVM respectively. Where, for the general case $\mathbf{B} = \mathbf{LN}$ and the general two dimensional differential operator $\mathbf{L}$ is described in Appendix D. The shape functions for CST elements are described in Appendix B and the plane stress or strain elasticity matrices and the general two dimensional normal operator $\mathbf{R}$ are also described in Appendix D.

Consider a collection of CST elements surrounding a node i, as illustrated in Figures 4.5a and 4.5b for the FEM and the FVM respectively. The kth component of the external force vector due to visco-plastic strains for the FEM with contributions from n_{el} elements is

$$f_{ik}^{fe} = -\sum_{e=1}^{n_{el}} \int_{\Omega_i^e} \frac{\partial N_i^e}{\partial x_j} D^e \epsilon_{vp_{jk}}^e \mathrm{d}\Omega = \sum_{e=1}^{n_{el}} D^e \epsilon_{vp_{jk}}^e \left(-\int_{\Omega_i^e} \frac{\partial N_i^e}{\partial x_j} \mathrm{d}\Omega \right) \tag{4.9}$$

at node i.

Alternatively, for the FVM it is

$$f_{ik}^{fv} = \sum_{e=1}^{n_{el}} \int_{\Gamma_i^e} n_j D^e \epsilon_{vp_{jk}}^e \mathrm{d}\Gamma = \sum_{e=1}^{n_{el}} D^e \epsilon_{vp_{jk}}^e \left(\int_{\Gamma_i^e} n_j \mathrm{d}\Gamma \right). \tag{4.10}$$

In both cases the visco-plastic strain tensor is constant over the element, thus allowing the visco-plastic strain factor to be taken outside of the integral. This is a consequence of

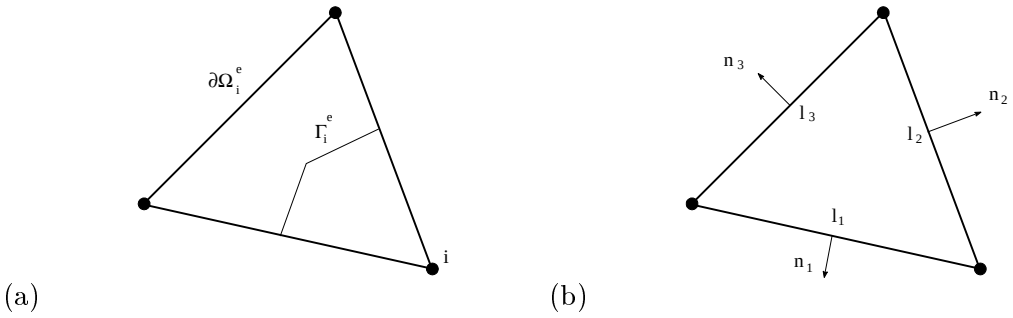

(a) (b)

Figure 4.6: Single CST (a) elemental contributions and (b) sides and lengths.

the linear nature of the element which furnishes strain and other associated constitutive variables as constants over the element.

Hence, the contributions for the two methods are identical if the bracketed integrals in equations 4.9 and 4.10 are equivalent. The equivalence of these two integrals has been comprehensively described by Oñate et al [71] in the analysis of elastic problems. The proof is also described here in order to provide a complete analysis of CST elements.

Concentrating on a single element, taken from the collection described in Figure 4.5a, it is possible to analyse the elemental contributions for the FEM and the FVM as illustrated in Figure 4.6a. The element is assumed to consist of sides of lengths l_1, l_2, l_3 and unit outward normals $\mathbf{n_1}, \mathbf{n_2}, \mathbf{n_3}$ as illustrated in Figure 4.6b. The boundary of the element is $\partial\Omega_i^e$ and the elemental contribution to the FVM control volume boundary is Γ_i^e.

Hence, the following derivation is possible:

$$\int_{\Omega_i^e} \frac{\partial N_i^e}{\partial x_j} \mathrm{d}\Omega = \int_{\partial\Omega_i^e} n_j N_i \mathrm{d}\Gamma = n_{1j}\frac{1}{2}l_1 + n_{2j}\frac{1}{2}l_2 = -\int_{\Gamma_i^e} n_j \mathrm{d}\Gamma \tag{4.11}$$

which is in essence obtained by application of the divergence theorem as described in Appendix A.

The direct equivalence of the two methods for problems involving material non-linearity is an important consideration and is further illustrated by the results obtained when modelling

two dimensional applications with CST elements. This equivalence will also be highlighted in the following chapter for a variety of numerical applications.

4.1.2.2 Bilinear quadrilateral elements

As for the previous CST elements, directly equivalent shape functions are utilised in the application of both the FEM and the FVM to describe the variation of the displacement over an element. The shape functions for bilinear quadrilateral (BLQ) elements are described in Appendix B.

The representation of BLQ elements in local coordinates is illustrated for the FEM and the FVM in Figures 4.7b and 4.7c respectively, both are representations of an arbitrarily deformed BLQ element in global coordinates as illustrated in Figure 4.7a. In the FEM case the BLQ element involves four Gauss points, similarly in the FVM four integration points are required to construct the associated sub-control volumes.

At present there is no accurate method available to analyse and compare the implementation of higher order two dimensional elements, such as BLQ elements. The previous method for CST elements relies on the fact that the strain and associated constitutive variables are constant over the element. This is not the case for BLQ elements, which by definition are bilinear as opposed to linear, and hence the strain and associated constitutive values vary linearly over the element. Though it is possible to assume that BLQ elements will approach a condition where there is limited variation of the constitutive variables over an element for a suitably refined mesh. Hence, indicating the equivalence of the two methods in that limit. Indeed, as indicated by the numerical results in the following chapter, this is apparently the case, but it does not provide a method of determining which method is superior or inferior with regard to accuracy.

It should be noted that for BLQ elements the FVM and the FEM will always provide distinctive elemental contributions.

Finally, the issue of asymmetric elemental stiffness contributions arises for non-orthogonal

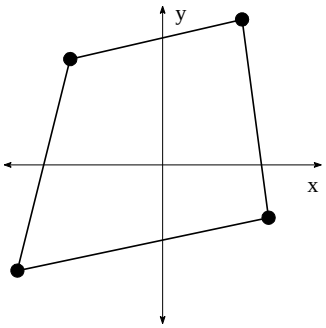

(a)

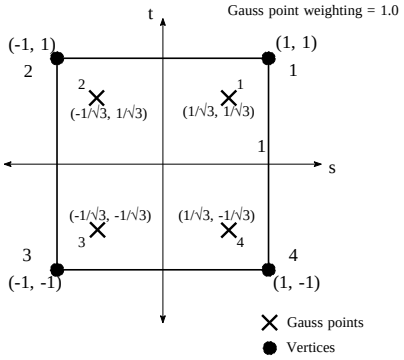

(b)

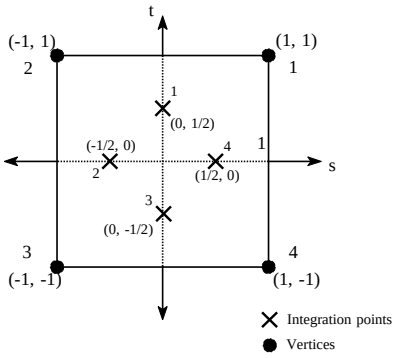

(c)

Figure 4.7: BLQ element. (a) Global, (b) FEM local and (c) FVM local coordinates.

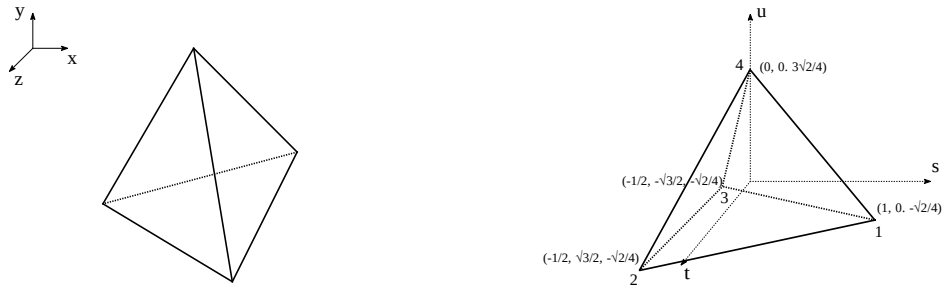

(a) (b)

Figure 4.8: Linear tetrahedral element in (a) global coordinates and (b) local coordinates.

BLQ elements. This leads to an asymmetric coefficient matrix, which requires specialised linear solvers. This is opposite to the FEM which will always produces a symmetric elemental stiffness contribution, regardless of the orthogonality of the element concerned. This issue will be further highlighted in the following chapter for a variety of numerical applications.

4.1.3 Three Dimensional Analysis

In this section the implementation of three dimensional elements in the FEM and the FVM will be described and compared. As in the case of the CST element, it is possible to analyse and compare the FVM and the FEM for the linear tetrahedral element. Unfortunately, as with BLQ elements in the two dimensional case no simple analytical comparison is available with regard to the higher order bilinear or trilinear elements in three dimensions, though the same arguments apply with regard to closer agreement of the two methods in the limit of a suitably refined mesh.

The three dimensional elements discussed in this section are illustrated in both global and local coordinates in Figures 4.8, 4.9 and 4.10 respectively. The element described in Figures 4.8a and 4.8b is the linear tetrahedral (LT) element, while the element described in Figures 4.9a and 4.9b is the bilinear pentahedral (BLP) or wedge element and the element described in Figures 4.10a and 4.10b is the trilinear hexahedral (TLH) or brick element.

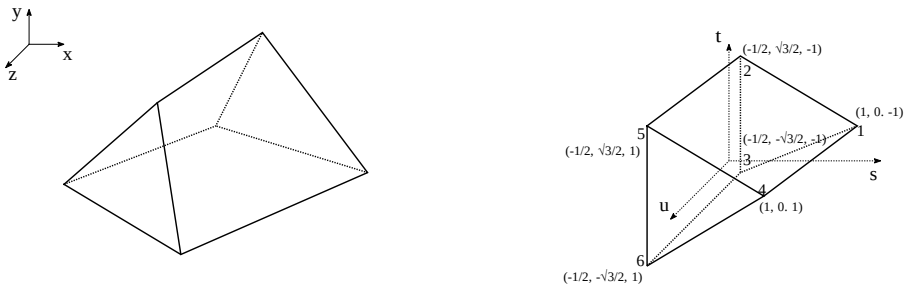

(a) (b)

Figure 4.9: Bilinear pentahedral element in (a) global coordinates and (b) local coordinates.

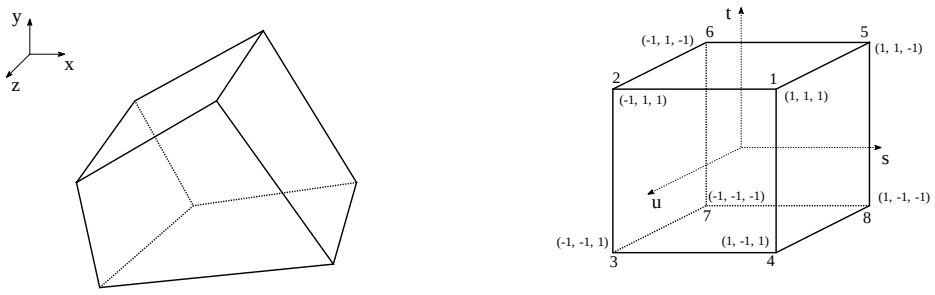

(a) (b)

Figure 4.10: Trilinear hexahedral element in (a) global coordinates and (b) local coordinates.

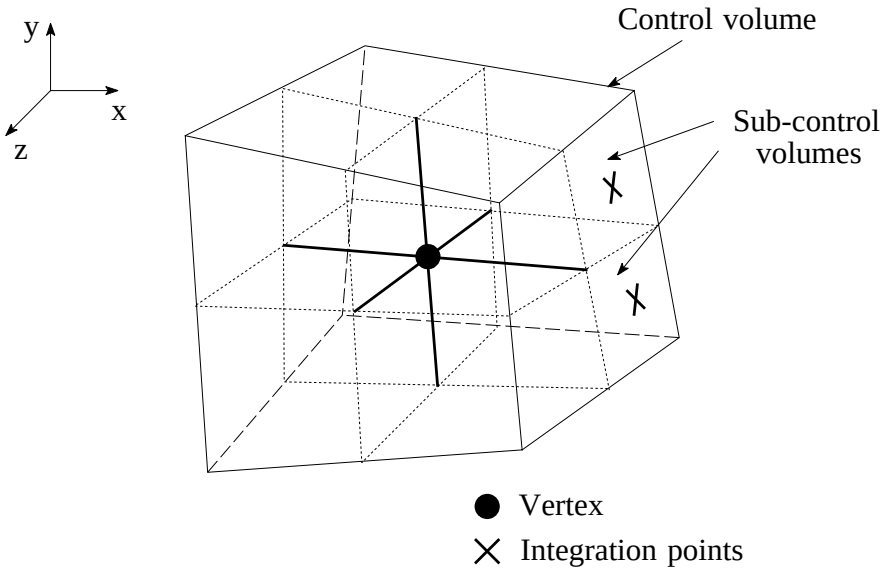

Figure 4.11: Three dimensional vertex based control volume.

As for the two dimensional case, directly equivalent meshes can be handled by the FEM and the FVM, though the stiffness matrix contributions are computed differently. Additionally, the global to local mapping of the elements again allows an arbitrarily deformed three dimensional element to be treated identically in computational terms.

For the FVM the construction of the sub-control volumes is a relatively straight forward extension of the two dimensional approach, except that in the three dimensional approach the control volumes are defined by internal surfaces of the mesh element. In this way it is possible to construct a control volume consisting of cubic sub-control volume contributions from associated elements.

This approach is illustrated in Figure 4.11 for the simple case of eight arbitrary elements contributing to a vertex based control volume. The control volume consists of the eight surrounding cubic sub-control volumes. Each sub-control volume has three integration points associated with it, which are situated at the face centres. It should be noted that it is possible to utilise a numerical integration scheme involving a greater number of weighted

integration points. Though this approach is relatively straight forward it has not been investigated in the research presented here, as it essentially involves the further comparison of the two methods for higher order numerical integration point schemes. This research is restricted to comparing equivalent lower order integration schemes for the two methods.

Finally, it should be noted that the case works equally well for a vertex with n associated elements, where n may consist of a variety of element types, such as tetrahedra, wedges or bricks.

4.1.3.1 Linear Tetrahedral elements

The shape functions associated with both the FVM and the FEM for linear tetrahedral (LT) elements are described in Appendix B. Naturally, as in the two dimensional case, the nodal points are equivalently defined in the local coordinate system for the FEM and the FVM. This is necessary in order to be consistent with the shape functions. The LT element is described in local coordinates in Figure 4.8b.

Obviously, the coordinates for the FEM Gauss points and the FVM integration points are different. To illustrate this difference the Gauss point for the FEM and the integration points for the FVM are described in Figure 4.12 and Figures 4.13 respectively. The six integration points for the FVM are illustrated in Figure 4.13a and Figure 4.13b, where as the single Gauss point is illustrated in Figure 4.12. The weighting associated with the Gauss point is equivalent to the volume the tetrahedron occupies in the local coordinate system.

For the FVM the six integration points coincide with the six internal surfaces required to construct the four cubic sub-control volumes associated with a LT element.

It is important to note that it is possible to analyse and compare the FVM and the FEM for the LT element due to its simple linear nature. It is possible to extend the previous two dimensional analysis of CST elements to the three dimensional analysis of LT elements.

The previous analysis was dimensionless upto the consideration of the equivalence of the

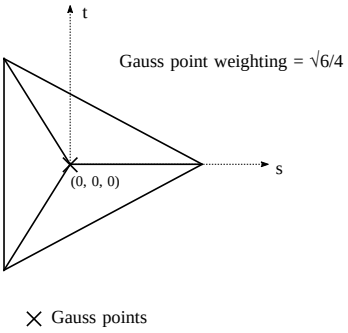

Figure 4.12: LT element Gauss point in local coordinates and associated weighting.

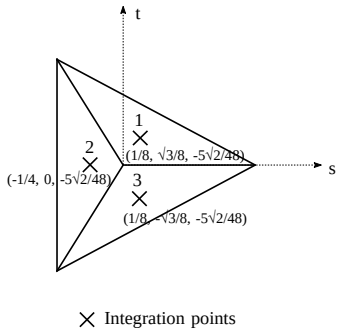

(a)

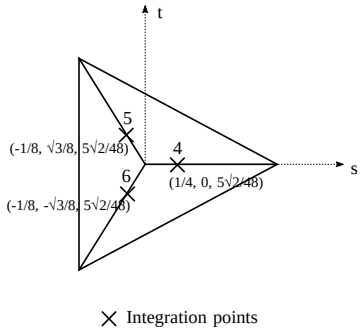

(b)

Figure 4.13: LT element integration points in local coordinates (a) vertical and (b) horizontally inclined.

two integrals as described in equations 4.9 and 4.10. It is further possible to prove the equivalence of these two integrals with regard to LT elements. Consider a cluster of LT elements surrounding the vertex i in a similar fashion to that described for CST elements in Figure 4.6(a).

In this three dimensional case it is possible to consider a single LT element from the cluster with surfaces of area s_1, s_2, s_3 and s_4 and unit outward normals $\mathbf{n_1}, \mathbf{n_2}, \mathbf{n_3}$ and $\mathbf{n_4}$.

Hence, extending the derivation described in equation 4.11 for CST elements to the case of LT elements it follows that

$$\int_{\Omega_i^e} \frac{\partial N_i^e}{\partial x_j} \mathrm{d}\Omega = \int_{\partial\Omega_i^e} n_j N_i \mathrm{d}\Gamma = n_{1j}\frac{1}{3}s_1 + n_{2j}\frac{1}{3}s_2 + n_{3j}\frac{1}{3}s_3 = -\int_{\Gamma_i^e} n_j \mathrm{d}\Gamma, \tag{4.12}$$

where $\partial\Omega_i^e$ remains the boundary of the element and Γ_i^e is the elemental contribution to the FVM control volume. It should be noted that the LT element is orientated such that surface s_4 is opposite vertex i.

4.1.3.2 Bilinear Pentahedral elements

The shape functions associated with both the FVM and the FEM for bilinear pentahedral (BLP) elements are described in Appendix B. The BLP element is described in local coordinates in Figure 4.9b.

The Gauss points for the FEM are described in Figures 4.14 and the integration points for the FVM are described in Figures 4.15. The nine integration points for the FVM are drawn in three planes, Figure 4.15a, Figure 4.15b and Figure 4.15c, where as the six Gauss points are drawn in two planes in Figure 4.14a and Figure 4.14b.

For the FVM the nine integration points coincide with the nine internal faces required to construct the six cubic sub-control volumes associated with a BLP element. The elemental stiffness matrices formed from a BLP element also distinctive for the two methods. Additionally, for the FVM an asymmetric elemental contribution is added to the coefficient matrix for BLP elements when the triangular faces are non-orthogonal or not equilateral,

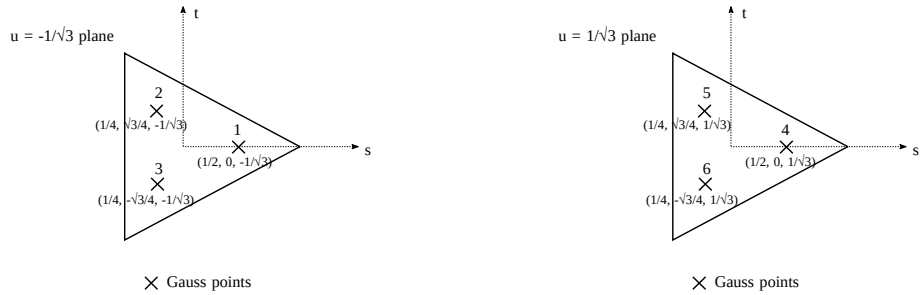

(a) (b)

Figure 4.14: BLP Gauss points in local coordinates. (a) $u = -1/\sqrt{3}$ and (b) $u = 1/\sqrt{3}$.

where as for the FEM the contributions are again always symmetric.

The consequence of this asymmetry is analysed and discussed with regard to linear solvers in the following chapters.

4.1.3.3 Trilinear Hexahedral elements

The shape functions associated with both the FVM and the FEM for trilinear hexahedral elements (TLH) are described in Appendix B. The TLH element is described in the local coordinate system in Figure 4.10b.

The twelve integration points for the FVM are drawn in three planes, Figures 4.17a, 4.17b and 4.17c, where as the eight Gauss points are drawn in two planes, Figures 4.16a and 4.16b.

For the FVM the twelve integration points coincide with the twelve internal surfaces required to construct the eight cubic sub-control volumes associated with a TLH element.

The elemental stiffness matrices formed from a TLH element are again different for the two methods. Additionally, for the FVM an asymmetric contribution to the coefficient matrix is provided for non-orthogonal elements, where as for the FEM the contributions are always

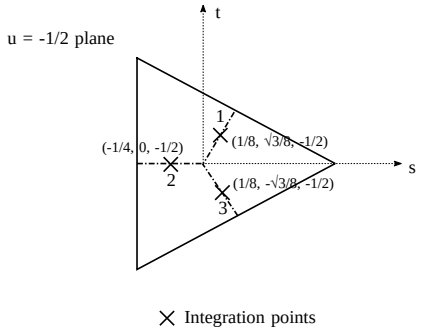

(a)

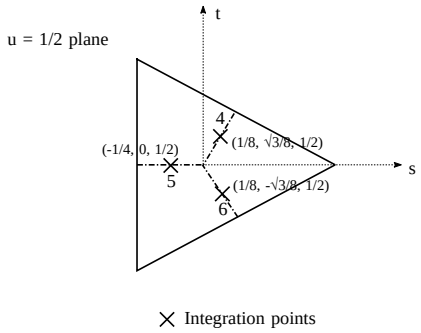

(b)

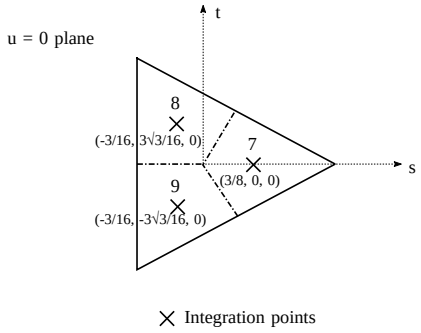

(c)

Figure 4.15: BLP FVM integration points in local coordinates. (a) $u = -\frac{1}{2}$, (b) $u = \frac{1}{2}$ and (c) $u = 0$ planes.

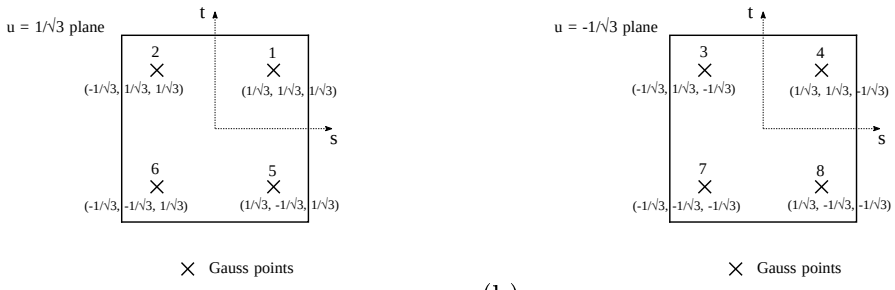

(a) (b)

Figure 4.16: TLH Gauss points in local coordinates. (a) $u = 1/\sqrt{3}$ and (b) $u = -1/\sqrt{3}$.

symmetric regardless of the orthogonality of the TLH element.

Again, the consequence of this asymmetry is analysed and discussed with regard to linear solvers in the following chapters.

4.2 Closure

In this chapter, a rudimentary theoretical comparison of the FVM and the FEM, when applied to problems involving material non-linearity, has been given. The direct equivalence of the two methods for the linear family of elements, which includes the one dimensional linear element, the two dimensional CST element and the three dimensional linear tetrahedral element have been illustrated and commented upon. At present, to the best of the authors knowledge, no definitive theoretical comparisons of higher order two or three dimensional elements has been performed, the difficulty being the bilinear and trilinear nature of the higher order elements, which furnishes linear or bilinear variation of the strain and other associated constitutive variables over the element concerned.

In the following chapter the two methods will be compared against a number of verification problems to complete the comparison.

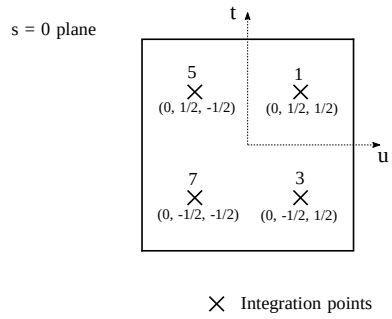

(a)

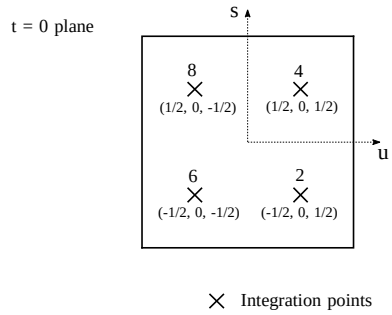

(b)

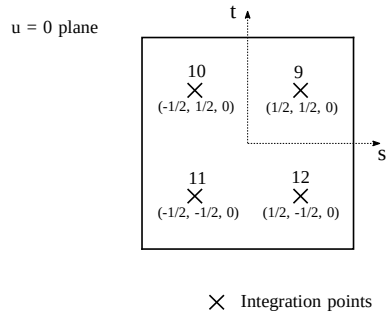

(c)

Figure 4.17: TLH FVM integration points in local coordinates. (a) u, (b) s and (c) t planes.